

# Detecting chiral pairing and topological superfluidity using circular dichroism

J. M. Midtgaard,<sup>1</sup> Zhigang Wu,<sup>2,3</sup> N. Goldman,<sup>4</sup> and G. M. Bruun<sup>1,2</sup>

<sup>1</sup>*Department of Physics and Astronomy, Aarhus University, Ny Munkegade, DK-8000 Aarhus C, Denmark.*

<sup>2</sup>*Shenzhen Institute for Quantum Science and Engineering and Department of Physics, Southern University of Science and Technology, Shenzhen 518055, China*

<sup>3</sup>*Center for Quantum Computing, Peng Cheng Laboratory, Shenzhen 518055, China*

<sup>4</sup>*Center for Nonlinear Phenomena and Complex Systems, Université Libre de Bruxelles, CP 231, Campus Plaine, 1050 Brussels, Belgium*

(Dated: September 11, 2020)

Realising and probing topological superfluids is a key goal for fundamental science, with exciting technological promises. Here, we show that chiral  $p_x + ip_y$  pairing in a two-dimensional topological superfluid can be detected through circular dichroism, namely, as a difference in the excitation rates induced by a clockwise and counter-clockwise circular drive. For weak pairing, this difference is to a very good approximation determined by the Chern number of the superfluid, whereas there is a non-topological contribution scaling as the superfluid gap squared that becomes significant for stronger pairing. This gives rise to a competition between the experimentally driven goal to maximise the critical temperature of the superfluid, and observing a signal given by the underlying topology. Using a combination of strong coupling Eliashberg and Berezinskii-Kosterlitz-Thouless theory, we analyse this tension for an atomic Bose-Fermi gas, which represents a promising platform for realising a chiral superfluid. We identify a wide range of system parameters where both the critical temperature is high and the topological contribution to the dichroic signal is dominant.

## I. INTRODUCTION

The realisation and manipulation of topological superfluids and superconductors is presently one of the most actively pursued goals in physics. In addition to being interesting from a fundamental science point of view, their Majorana edge modes promise applications for quantum computing [1]. Zero-energy states at the ends of one-dimensional (1D) nanowires have been observed, consistent with the presence of Majorana modes [2, 3]. So far, there has however been no observation of topological superfluidity in 2D. The most promising solid-state candidate for a 2D topological superconductor is  $\text{Sr}_2\text{RuO}_4$ , but the precise symmetry of the order parameter in this crystal remains subject to intense debate [4–6]. It has recently been shown that an atomic 2D Fermi gas immersed in a BEC offers a promising platform for realising a topological superfluid [7–9]. The fermions form Cooper pairs with chiral symmetry by exchanging sound modes in the BEC, and the system offers sufficient flexibility so that one can tune the superfluid critical temperature to be within experimental reach. Experimentally, such a Bose-Fermi mixture has been realized using  $^{173}\text{Yb}$ - $^7\text{Li}$  atoms, which constitutes an important step towards the first unequivocal realisation of a topological  $p_x + ip_y$  superfluid [10].

A key question concerns the detection of topological superfluidity in atomic gases. Their topological properties are not easily extracted from thermodynamic measurements nor using common probes such as radio-frequency spectroscopy [11]. Contrary to the chiral edge modes of single-particle band structures, which have been detected in experiments [12], the observation of Majorana states [13, 14] is complicated by their small number and their particle-hole nature.

It was recently proposed [15, 16] and experimentally demonstrated [17] that the topologically invariant Chern number can be detected in atomic gases through circular dichroism, namely, by analyzing excitation rates upon applying a circular drive. This topological probe was first introduced for non-interacting Chern insulators [15], and later applied to interacting many-body systems [18–20]. Inspired by this approach, we hereby demonstrate that the chirality of the  $p_x + ip_y$  pairing is revealed in the circular dichroism of the superfluid. For weak pairing, the differential excitation rate obtained from opposite drive orientations, integrated over the drive frequency, is shown to be determined by the Chern number of the topological superfluid, in direct analogy with Chern insulators [15]. However, in contrast with the latter case, a non-topological contribution scaling as the superfluid gap squared becomes significant for strong pairing. The resulting competition between maximising the superfluid critical temperature while detecting a genuine topological signature is analysed for a concrete atomic Bose-Fermi mixture. Using the strong-coupling Eliashberg equations combined with Berezinskii-Kosterlitz-Thouless (BKT) theory, we identify a wide and accessible parameters regime where the superfluid critical temperature is high and the dichroic signal dominated by the topological Chern number. Our results demonstrate that the dichroic probe offers an experimentally promising pathway to detect topological superfluidity.

## II. TOPOLOGICAL RESPONSES IN SUPERFLUIDS

We first establish a connection between circular dichroism, the Hall conductivity, and the Chern number of

the superfluid. Consider a 2D system of spin-polarised fermions described by the Hamiltonian

$$H_0 = \int d^2r \psi^\dagger(\mathbf{r}) \left( -\frac{\nabla^2}{2m} \right) \psi(\mathbf{r}) + \frac{1}{2} \iint d^2r d^2r' \psi^\dagger(\mathbf{r}) \psi^\dagger(\mathbf{r}') V(\mathbf{r} - \mathbf{r}') \psi(\mathbf{r}') \psi(\mathbf{r}), \quad (1)$$

where  $\psi(\mathbf{r})$  is the fermion field and  $V(\mathbf{r} - \mathbf{r}')$  is an interaction giving rise to pairing, which may result from a  $p$ -wave Feshbach resonance or, as we will consider later, from an induced interaction. Within BCS theory, this  $p$ -wave superfluid can be described by the Hamiltonian

$$H_{\text{BCS}} = \sum_{\mathbf{k}} \Phi_{\mathbf{k}}^\dagger H_{\mathbf{k}} \Phi_{\mathbf{k}}, \quad H_{\mathbf{k}} = \mathbf{h}_{\mathbf{k}} \cdot \boldsymbol{\tau}, \quad (2)$$

where  $\Phi_{\mathbf{k}} \equiv [a_{\mathbf{k}}, a_{-\mathbf{k}}^\dagger]^T$ ,  $\mathbf{h}_{\mathbf{k}} = (\text{Re}\Delta_{\mathbf{k}}, -\text{Im}\Delta_{\mathbf{k}}, \xi_{\mathbf{k}})^T$  and where  $\boldsymbol{\tau} = (\tau_1, \tau_2, \tau_3)^T$  with  $\tau_i$  the Pauli matrices. Here  $\xi_{\mathbf{k}} = k^2/2m - \mu$ , where  $\mu$  is the chemical potential, and  $\Delta_{\mathbf{k}}$  is the gap parameter ( $\hbar=1$  throughout). The latter is taken to have chiral  $p$ -wave symmetry, i.e.  $\Delta_{\mathbf{k}} = \Delta_k e^{i\phi}$ , where  $\phi$  is the polar angle of the momentum  $\mathbf{k}$  and  $k = |\mathbf{k}|$ , since this gives the lowest energy for  $p$ -wave pairing as it have no nodes [21, 22]. Indeed, as  $\Delta_k \propto k$  for  $k \ll k_F$  due to Fermi anti-symmetry, we get  $\Delta_{\mathbf{k}} \propto k_x + ik_y$ . This results in a topological phase characterised by a Chern number  $C = -1$  for  $\mu > 0$  whereas  $C = 0$  for  $\mu < 0$  [23]. The Chern number reads

$$C = \int \frac{d^2k}{4\pi} \frac{1}{|\mathbf{h}_{\mathbf{k}}|^3} \mathbf{h}_{\mathbf{k}} \cdot \partial_{k_x} \mathbf{h} \times \partial_{k_y} \mathbf{h} \quad (3) = \int \frac{d^2k}{2\pi} \left[ \frac{v_x}{E_{\mathbf{k}}^3} \text{Im}(\Delta_{\mathbf{k}}^* \partial_{k_y} \Delta_{\mathbf{k}}) + \frac{\xi_{\mathbf{k}}}{2E_{\mathbf{k}}^3} \text{Im}(\partial_{k_x} \Delta_{\mathbf{k}} \partial_{k_y} \Delta_{\mathbf{k}}^*) \right],$$

where  $v_x = k_x/m$  and  $E_{\mathbf{k}} = \sqrt{\xi_{\mathbf{k}}^2 + |\Delta_{\mathbf{k}}|^2}$  is the BCS quasiparticle energy. The second term in the integrand scales as  $\Delta_{\mathbf{k}}^2/\mu^2$  so that the Chern number can be approximated by the first term in the regime  $\Delta_{\mathbf{k}} \ll \mu$ .

We now show that the Chern number in Eq. (3) can be extracted from circular dichroism, namely, by monitoring excitation rates upon a circular drive [15, 17]. We consider a circular drive of the form

$$V_{\pm}(\mathbf{r}; \mathbf{q}) = 2\mathcal{E} (x \cos \Omega t \pm y \sin \Omega t) \cos \mathbf{q} \cdot \mathbf{r}, \quad (4)$$

and we will set  $\mathbf{q} \rightarrow 0$  at the end of calculations, corresponding to a uniform circular shaking [17]. This reads

$$V_{\pm}(\mathbf{q}) = \frac{\mathcal{E}}{i} \left[ -\frac{\partial \tilde{n}(\mathbf{q})}{\partial q_x} \pm i \frac{\partial \tilde{n}(\mathbf{q})}{\partial q_y} \right] e^{-i\Omega t} + \text{h.c.}, \quad (5)$$

in second quantization, where  $n(\mathbf{r}) = \psi^\dagger(\mathbf{r})\psi(\mathbf{r})$  is the density operator,  $n(\mathbf{q})$  is its Fourier transform and  $\tilde{n}(\mathbf{q}) = [n(\mathbf{q}) - n(-\mathbf{q})]/2$ . Within linear response, the excitation rate out of the ground state of  $H_0$  induced by  $V_{\pm}(\mathbf{q})$  can be calculated using Fermi's golden rule as

$$\Gamma_{\pm}(\mathbf{q}, \Omega) = 2\pi \mathcal{E}^2 \sum_f \left| \left\langle f \left| \frac{\partial \tilde{n}(\mathbf{q})}{\partial q_x} \pm i \frac{\partial \tilde{n}(\mathbf{q})}{\partial q_y} \right| g \right\rangle \right|^2 \times \delta(E_f - E_g - \Omega), \quad (6)$$

where  $|g\rangle$  and  $|f\rangle$  denote the ground and excited states of  $H_0$  with energy  $E_g$  and  $E_f$ , respectively.

The observable of interest is provided by the differential integrated rate (DIR), which is defined as [15]

$$\Delta\Gamma = \lim_{\mathbf{q} \rightarrow 0} \frac{1}{2} \int_0^\infty d\Omega [\Gamma_+(\mathbf{q}, \Omega) - \Gamma_-(\mathbf{q}, \Omega)]. \quad (7)$$

Substituting Eq. (6) into Eq. (7), we find

$$\Delta\Gamma = -\pi i \mathcal{E}^2 \lim_{\mathbf{q} \rightarrow 0} \left\langle g \left[ \left[ \frac{\partial n(\mathbf{q})}{\partial q_x}, \frac{\partial n(-\mathbf{q})}{\partial q_y} \right] \right] g \right\rangle, \quad (8)$$

where we have used momentum conservation to eliminate terms. We now use the continuity equation to write  $\Delta\Gamma$  in terms of the density-current correlation function. From  $\partial_t n(\mathbf{r}, t) + \nabla \cdot \mathbf{j}(\mathbf{r}, t) = 0$ , we find

$$\langle g | n(\mathbf{q}) | f \rangle = \frac{\langle g | \mathbf{q} \cdot \mathbf{j}(\mathbf{q}) | f \rangle}{E_f - E_g}, \quad (9)$$

where the Fourier transform of the current reads

$$\mathbf{j}(\mathbf{q}) = (1/2mi) \int d^2r e^{-i\mathbf{q} \cdot \mathbf{r}} [\psi^\dagger(\mathbf{r}) \nabla \psi(\mathbf{r}) - \text{h.c.}]. \quad (10)$$

Using Eqs. (8)-(9) and noting that

$$\lim_{q_y \rightarrow 0} \lim_{q_x \rightarrow 0} \langle g | \partial_{q_y} n(\mathbf{q}) | f \rangle = \lim_{q_y \rightarrow 0} \lim_{q_x \rightarrow 0} \langle g | n(\mathbf{q}) / q_y | f \rangle, \quad (11)$$

we find the relation

$$\Delta\Gamma / \mathcal{A} = 2\pi \mathcal{E}^2 \sigma_{xy}, \quad (12)$$

which connects the DIR to the static Hall conductivity

$$\sigma_{xy} \equiv \lim_{q_y \rightarrow 0} \lim_{q_x \rightarrow 0} \lim_{\omega \rightarrow 0} \frac{1}{i\mathcal{A}\omega} \chi_{j_x, j_y}(\mathbf{q}, \omega) = \lim_{q_y \rightarrow 0} \lim_{q_x \rightarrow 0} \lim_{\omega \rightarrow 0} \frac{1}{i\mathcal{A}q_y} \chi_{j_x, n}(\mathbf{q}, \omega). \quad (13)$$

Here  $\mathcal{A}$  is the system's area, and  $\chi_{A,B}(\mathbf{q}, \omega)$  is the Fourier transform of the retarded correlation function

$$\chi_{A,B}(\mathbf{q}, t - t') = -i\theta(t - t') \langle [A(\mathbf{q}, t), B(-\mathbf{q}, t')] \rangle, \quad (14)$$

with  $\theta(x)$  the Heaviside function. We note that the specific order of limits (taking  $\omega \rightarrow 0$  before  $\mathbf{q} \rightarrow 0$ ) is crucial, since the more standard order  $\lim_{\omega \rightarrow 0} \lim_{\mathbf{q} \rightarrow 0} \frac{1}{i\omega} \chi_{j_x, j_y}(\mathbf{q}, \omega)$  yields zero for a translationally invariant system [25]; this subtlety also arises when analysing edge currents [26-29].

Besides, Eq. (12) was obtained by taking the finite nature of realistic systems into account. In particular, one would obtain an additional factor of 1/2 for a strictly translationally invariant system. Indeed, when deriving Eq. (8), we use that  $\langle A(\mathbf{q}), B(\mathbf{q}') \rangle \propto \delta_{\mathbf{q}, -\mathbf{q}'}$  for a strictly infinite translationally invariant system. From this, it follows that  $\lim_{\mathbf{q} \rightarrow 0} \langle n(\mathbf{q}) n(\mathbf{q}) \rangle = 0$  and such terms can be discarded. However, for a finite physical system of size  $L$ , momentum is only defined with a resolution  $\sim 1/L$ . This

means that  $\langle n(\mathbf{q})n(\mathbf{q}) \rangle$  starts to become non-zero for  $q \lesssim 1/L$  and in particular  $\lim_{\mathbf{q} \rightarrow 0} \langle n(\mathbf{q})n(\mathbf{q}) \rangle = \langle n(\mathbf{0})n(\mathbf{0}) \rangle$  for a finite system, which leads to the extra factor of 2 on the right hand side of Eq. (12). Physically, it means that a finite system cannot distinguish between a force with wave length much greater than the system size from a uniform force. We note that uniform circular shaking ( $\mathbf{q}=0$ ) can be realized in ultracold-atom experiments. We also point out that Eq. (12) is universal: it can also be derived from Kramers-Kronig relations [15, 19, 30, 31], noting that the excitation rates  $\Gamma_{\pm}(\Omega)$  are related to the power absorbed upon the circular drive  $P_{\pm}(\Omega) = \Omega \Gamma_{\pm}(\Omega)$ .

The Hall conductivity of a superfluid was previously shown to be related to a Chern number; see Refs. [26, 27] in the context of chiral  $^3\text{He}$  superfluids. Using BCS theory, the current-density correlation function can be written as [41]

$$\chi_{j_x, n}(q) = - \sum_k \frac{k_x}{2m} \text{tr} [\mathcal{G}_0(k - q/2) \mathcal{G}_0(k + q/2) \tau_3] \quad (15)$$

where in shorthand notation  $k = (\mathbf{k}, \omega_n)$  with  $\omega_n$  a fermionic Matsubara frequency, and  $\mathcal{G}_0$  is the BCS Green's function. We have

$$\mathcal{G}_0(k) = \int_{-\infty}^{\infty} \frac{d\omega}{(-\pi)} \frac{\text{Im} \mathcal{G}_0(\mathbf{k}, \omega)}{i\omega_n - \omega} \quad (16)$$

where

$$\begin{aligned} \text{Im} \mathcal{G}_0(\mathbf{k}, \omega) = & - \frac{\pi}{2E_{\mathbf{k}}} \begin{pmatrix} \omega + \xi_{\mathbf{k}} & -\Delta_{\mathbf{k}} \\ -\Delta_{\mathbf{k}}^* & \omega - \xi_{\mathbf{k}} \end{pmatrix} \\ & \times [\delta(\omega - E_{\mathbf{k}}) - \delta(\omega + E_{\mathbf{k}})]. \end{aligned} \quad (17)$$

Inserting this in Eq. (15) and performing the Matsubara sum yields to first order in  $\mathbf{q}$

$$\begin{aligned} \lim_{\mathbf{q} \rightarrow 0} \chi_{j_x, n}(\mathbf{q}, \omega) = & - \frac{iq_x}{\mathcal{V}} \sum_{\mathbf{k}} \frac{k_x}{2m} \frac{\text{Im} \Delta_{\mathbf{k}} \partial_{k_x} \Delta_{\mathbf{k}}^*}{E_{\mathbf{k}}^3} \\ & - \frac{iq_y}{2\mathcal{V}} \sum_{\mathbf{k}} \frac{k_x}{2m} \frac{\text{Im} \Delta_{\mathbf{k}} \partial_{k_y} \Delta_{\mathbf{k}}^*}{E_{\mathbf{k}}^3}. \end{aligned} \quad (18)$$

The first of these terms vanish, since the summand is odd in  $k_y$ . This can be seen if we fix the phase of the gap function and look at, for instance, the simple example  $\Delta_{\mathbf{k}} = k_x + ik_y$ . With this, it is clear that

$$\begin{aligned} \lim_{\mathbf{q} \rightarrow 0} \lim_{\omega \rightarrow 0} \frac{\chi_{j_x, n}(\mathbf{q}, \omega)}{iq_y} = & \int \frac{d^2 \mathbf{k}}{8\pi^2} \frac{k_x}{m} \frac{\text{Im} [\Delta_{\mathbf{k}}^* \partial_{k_y} \Delta_{\mathbf{k}}]}{E_{\mathbf{k}}^3} \\ = & \frac{C}{4\pi} + \mathcal{O}(\Delta^2/\mu^2), \end{aligned} \quad (19)$$

where the last equality is obtained by comparing with the Chern number in Eq. (3). In contrast with the case of Chern insulators, where the Hall conductivity is genuinely topological in the thermodynamic limit [32], the Hall response of the superfluid [Eq. (19)] contains a correction scaling as  $\mathcal{O}(\Delta^2/\mu^2)$ . This result was previously

related to the fact that the edge current of a chiral  $p$ -wave superconductor is not strictly topological, as opposed to the presence of edge (Majorana) states [33–35].

Finally, combining Eqs. (12) and (19) yields the central result of this work,

$$\Delta\Gamma/A = (1/2) \mathcal{E}^2 C + \mathcal{O}(\Delta^2/\mu^2), \quad (20)$$

which shows that the DIR related to the dichroic probe is closely related to the Chern number of the superfluid phase: this observable exhibits a jump proportional to the Chern number to order  $\mathcal{O}(\Delta^2/\mu^2)$  whenever the superfluid enters the topological phase with  $C = -1$ .

### III. DICHOIC PROBE FOR A TOPOLOGICAL BOSE-FERMI MIXTURE

We now explore the dichroic probe for a concrete system consisting of a 2D gas of fermionic atoms immersed in a 3D BEC. The fermions interact by exchanging sound modes in the BEC, which leads to an induced attractive interaction and Cooper pairing [7]. Since both the range and strength of the induced interaction can be varied, one can tune the mixture in order to reach a high critical temperature. This makes such a mixture a strong candidate for observing a chiral pairing. Recently, progress towards realising this goal was reported with the experimental realisation of a  $^{173}\text{Yb}$ - $^7\text{Li}$  mixture [10]. We now analyse how the dichroic probe can be used to detect topological pairing in this specific system.

Due to the finite speed of sound in the BEC, the interaction between the fermions mediated by the bosons is not instantaneous, thus giving rise to retardation effects. The latter are included in the frequency-dependent Eliashberg equations as explained in the appendix. It has been shown that retardation effects are small when the bosons in the BEC are light compared to the fermions such as for the  $^{173}\text{Yb}$ - $^7\text{Li}$  mixture [36]. The induced interaction is then close to the static Yukawa form

$$V(\mathbf{r}) = - \frac{a_{\text{eff}}^2 n_B m_B}{\pi} \frac{\exp(-\sqrt{2}r/\xi_B)}{r}. \quad (21)$$

Here,  $n_B$  and  $m_B$  is the density and mass of the bosons,  $\xi_B = 1/\sqrt{8\pi n_B a_B}$  is the BEC healing length with  $a_B$  the boson-boson scattering length, and  $a_{\text{eff}}$  is the mixed dimensional Bose-Fermi scattering length.

According to Eq. (7), one should measure the differential rate  $\Gamma_+ - \Gamma_-$  integrated over all frequencies. However, any real measurement necessarily introduces an upper cut-off frequency  $\Omega_c$  above which there is no signal [17]. Using Eqs. (12) and (19), the resulting signal reads

$$\frac{\Delta\Gamma_{\text{trunc}}(\Omega_c)}{\mathcal{A}\mathcal{E}^2} \equiv \int \frac{d^2 k}{4\pi} \frac{k_x}{m} \frac{\text{Im} [\Delta_{\mathbf{k}}^* \partial_{k_y} \Delta_{\mathbf{k}}]}{E_{\mathbf{k}}^3} \theta(\Omega_c - 2E_{\mathbf{k}}) \quad (22)$$

The cut-off  $\theta(\Omega_c - 2E_{\mathbf{k}})$  reflects that the probe breaks pairs with energy  $2E_{\mathbf{k}}$  in the long wave length limit. We note that  $\Delta\Gamma = \lim_{\Omega_c \rightarrow \infty} \Delta\Gamma_{\text{trunc}}(\Omega_c)$ .

In Fig. 1, we plot  $\Delta\Gamma_{\text{trunc}}(\Omega_c)$  for a  ${}^7\text{Li}-{}^{173}\text{Yb}$  mixture with a Bose-Fermi coupling  $n_B^{1/3} a_{\text{eff}} = 0.12$ , BEC gas parameter  $n_B^{1/3} a_B = 0.1$ , and density ratio  $n_F^{1/2}/n_B^{1/3} = 0.5$ , where  $n_F$  is the 2D Fermi density. These results are obtained by first solving the BCS equations self-consistently at zero temperature and then evaluating the DIR from Eq. (22). The numerical solution indeed confirms the  $p$ -wave form of pairing  $\Delta_{\mathbf{k}} = \Delta_k e^{i\phi}$  where  $\Delta_k \propto k$  for small momenta. The DIR is zero for cut-off frequencies

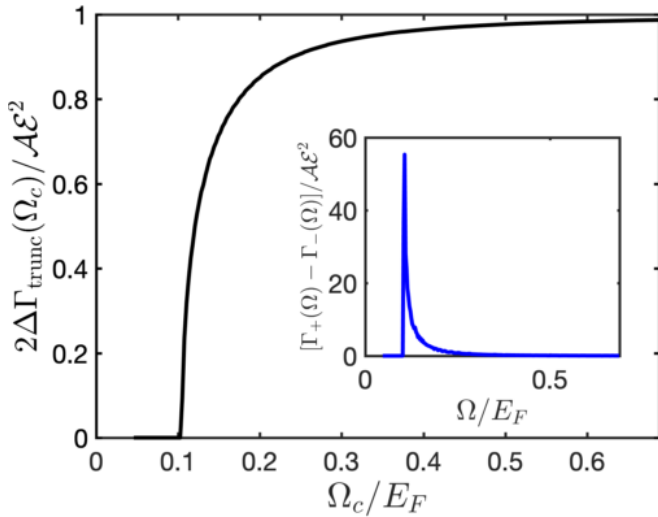


FIG. 1. (Color online). The differential integrated rate  $\Delta\Gamma_{\text{trunc}}(\Omega)$  between a clockwise and counterclockwise perturbation as a function of the cut-off frequency. The insert shows the difference in the heating rates between a clockwise and counterclockwise perturbation as a function of frequency.

below twice the gap, i.e. for  $\Omega_c \lesssim 0.1E_F$  where  $E_F$  is the 2D Fermi energy, reflecting that there is not enough energy in the probe to break pairs. Above this threshold, the DIR quickly converges towards to the Chern number for  $\Omega_c \gtrsim E_F$ . Since  $\Delta \simeq 0.05E_F \ll E_F$  for this set of parameters, the deviation of  $2\Delta\Gamma/A\mathcal{E}^2$  away from the Chern number is small. We also plot in Fig. 1 the differential rate at a given frequency  $\Omega$ ,

$$\frac{1}{2}[\Gamma_+(\Omega) - \Gamma_-(\Omega)] = \frac{\partial}{\partial\Omega} \Delta\Gamma_{\text{trunc}}(\Omega). \quad (23)$$

This difference is large for frequencies just above the threshold given by twice the gap, where the density of states of the superfluid is highest, and Fig. 1 shows that that one only needs to measure the difference up to a few times the pairing gap to resolve the Chern number.

One of the appealing features of the Bose-Fermi mixture is that the critical temperature for the 2D superfluid can be tuned to be close to the maximum value  $T_c/T_F = 1/16$  allowed by BKT theory. Maximising  $T_c$  will however also increase the gap and thereby increase corrections to the DIR away from the Chern number as seen from Eq. (20). To analyse this tension, we plot in Fig. 2 the DIR  $\Delta\Gamma$  at zero temperature and the critical

temperature  $T_c$  as a function of the gas parameter  $n_B^{1/3} a_B$  for  $n_F^{1/2}/n_B^{1/3} = 0.5$  and two different Bose-Fermi interaction strengths. The critical temperature is calculated by combining strong coupling Eliashberg and BKT theory, which includes the frequency dependence of the gap; see Refs. [7] and the appendix for details. We see that the critical temperature increases with decreasing gas parameter reflecting that the range of interaction in Eq. (21), given by the BEC coherence length, increases. The gap consequently also increases leading to a larger correction term for the DIR away from  $\Delta\Gamma = A\mathcal{E}^2\mathcal{C}/2$ . Nevertheless, Fig. 2 shows that there is a significant region where both the DIR is close to the topological value and the critical temperature is close to its maximum value  $T_c/T_F = 1/16$ . Note that we expect our calculation to give a lower bound on the DIR, since BCS theory likely overestimates the gap.

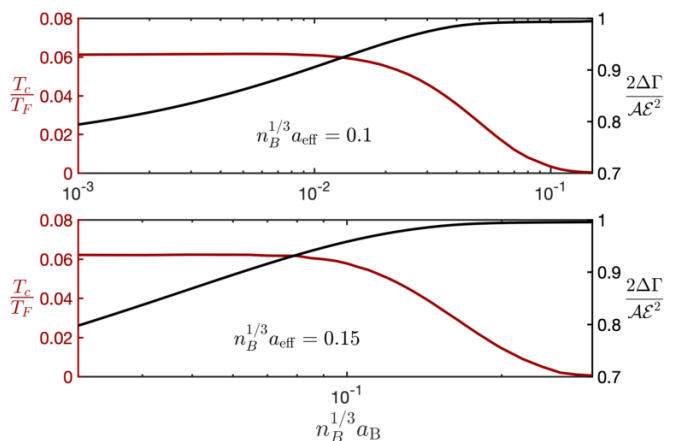


FIG. 2. (Color online). The critical temperature (red) and the differential integrated rate  $\Delta\Gamma$  (black) as a function of the BEC gas parameter  $n_B^{1/3} a_B$  for two different Bose-Fermi interaction strengths.

To further illustrate the competition between maximising the critical temperature and measuring a value of  $\Delta\Gamma$  determined by the underlying topology, we plot  $\Delta\Gamma$  at zero temperature as a function of  $T_c$  in Fig. 3 for the same parameters as in Fig. 2. This demonstrates that in order for the dichroic probe to yield a value close to that given by the Chern number, one should cool to around  $T \sim 0.06E_F$ . Since temperatures down to  $T \simeq 0.03E_F$  have been obtained for 2D Fermi gases [37–39], this is within present day technology making our scheme promising for detecting topological superfluidity. It also shows that a stronger Bose-Fermi interaction strength is slightly more favorable although the difference between the two interaction strengths is small.

For  $T = 0$ , BCS theory has been shown to be surprisingly accurate even for strong coupling where the Cooper pairs are tightly bound and the system is in the so-called BEC regime [40]. It follows that our calculation of the DIR is reliable even in this regime, where the correction term  $\mathcal{O}(\Delta^2/\mu^2)$  away from the quantized value is large.

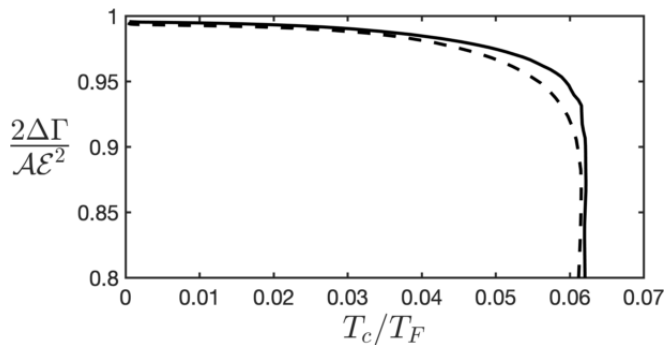


FIG. 3. The DIR as a function of the critical temperature for the same parameters as in Fig. 2. The dashed line corresponds to  $n_B^{1/3} a_{\text{eff}} = 0.1$  and the solid line to  $n_B^{1/3} a_{\text{eff}} = 0.15$ .

Any non-zero value however indicates chiral pairing, since the DIR is zero in a phase with time-reversal symmetry. Our scheme thus provides a way to observe the topological phase transition to a trivial phase when  $\mu$  becomes negative deep in the BEC regime.

#### IV. CONCLUSION

We showed that chiral  $p_x + ip_y$  pairing in a 2D superfluid can be detected through circular dichroism. Con-

trary to the case of topological insulators [15], the DIR is not purely dictated by the Chern number due to a correction term scaling as  $\Delta^2/E_F^2$ , giving rise to a competition between maximising the critical temperature of the superfluid and observing the Chern number from such a dichroic probe. As a concrete example, we considered an atomic Bose-Fermi mixture. Using a combination of Eliashberg and BKT theory, it was demonstrated that there is in fact a wide range of values for the system parameters where both the critical temperature is high and the dichroic signal close to the value given by the Chern number. This combined with the fact that a similar scheme was recently successfully applied to detect topological order in a Chern Bloch band [17], leads to the conclusion that the dichroic probe is a strong candidate for detecting topological  $p_x + ip_y$  pairing in an atomic system.

*Acknowledgements.* — J.M.M. and G.M.B. wish to acknowledge the support of the Danish Council of Independent Research – Natural Sciences via Grant No. DFF - 4002-00336. Z.W. acknowledges the support by the National Science Foundation of China (Grant No.11904417) and the Key-Area Research and Development Program of Guangdong Province (Grant No.2019B030330001). N.G. is supported by the ERC Starting Grant TopoCold, and the Fonds De La Recherche Scientifique (FRS-FNRS, Belgium).

- 
- [1] C. Nayak, S. H. Simon, A. Stern, M. Freedman, and S. Das Sarma, *Rev. Mod. Phys.* **80**, 1083 (2008).
  - [2] S. Nadj-Perge, I. K. Drozdov, J. Li, H. Chen, S. Jeon, J. Seo, A. H. MacDonald, B. A. Bernevig, and A. Yazdani, *Science* **346**, 602 (2014), <https://science.sciencemag.org/content/346/6209/602.full.pdf>.
  - [3] R. M. Lutchyn, E. P. A. M. Bakkers, L. P. Kouwenhoven, P. Krogstrup, C. M. Marcus, and Y. Oreg, *Nature Reviews Materials* **3**, 52 (2018).
  - [4] C. W. Hicks, J. R. Kirtley, T. M. Lippman, N. C. Koshnick, M. E. Huber, Y. Maeno, W. M. Yuhasz, M. B. Maple, and K. A. Moler, *Phys. Rev. B* **81**, 214501 (2010).
  - [5] A. P. Mackenzie, T. Scaffidi, C. W. Hicks, and Y. Maeno, *npj Quantum Materials* **2**, 40 (2017).
  - [6] S. A. Kivelson, A. C. Yuan, B. Ramshaw, and R. Thomale, *npj Quantum Materials* **5**, 43 (2020).
  - [7] Z. Wu and G. M. Bruun, *Phys. Rev. Lett.* **117**, 245302 (2016).
  - [8] J. M. Midtgaard, Z. Wu, and G. M. Bruun, *Phys. Rev. A* **94**, 063631 (2016).
  - [9] J. M. Midtgaard, Z. Wu, and G. M. Bruun, *Phys. Rev. A* **96**, 033605 (2017).
  - [10] F. Schäfer, N. Mizukami, P. Yu, S. Koibuchi, A. Bouscal, and Y. Takahashi, *Phys. Rev. A* **98**, 051602 (2018).
  - [11] E. Grosfeld, N. R. Cooper, A. Stern, and R. Ilan, *Phys. Rev. B* **76**, 104516 (2007).
  - [12] N. R. Cooper, J. Dalibard, and I. B. Spielman, *Rev. Mod. Phys.* **91**, 015005 (2019).
  - [13] G. Möller, N. R. Cooper, and V. Gurarie, *Phys. Rev. B* **83**, 014513 (2011).
  - [14] M. Gong, G. Chen, S. Jia, and C. Zhang, *Phys. Rev. Lett.* **109**, 105302 (2012).
  - [15] D. T. Tran, A. Dauphin, A. G. Grushin, P. Zoller, and N. Goldman, *Science Advances* **3** (2017), 10.1126/sciadv.1701207, <https://advances.sciencemag.org/content/3/8/e1701207.full.pdf>.
  - [16] D.-T. Tran, N. R. Cooper, and N. Goldman, *Physical Review A* **97**, 061602 (2018).
  - [17] L. Asteria, D. T. Tran, T. Ozawa, M. Tarnowski, B. S. Rem, N. Fläschner, K. Sengstock, N. Goldman, and C. Weitenberg, *Nature Physics* **15**, 449 (2019).
  - [18] M. Schüler and P. Werner, *Physical Review B* **96**, 155122 (2017).
  - [19] C. Repellin and N. Goldman, *Physical review letters* **122**, 166801 (2019).
  - [20] P. W. Klein, A. G. Grushin, and K. L. Hur, *arXiv preprint arXiv:2002.01742* (2020).
  - [21] P. W. Anderson and P. Morel, *Phys. Rev.* **123**, 1911 (1961).
  - [22] J. P. Lu and W. Barford, *Phys. Rev. B* **44**, 5263 (1991).
  - [23] N. Read and D. Green, *Phys. Rev. B* **61**, 10267 (2000).
  - [24] See *Supplemental Material* online for details.
  - [25] G. Giuliani and G. Vignale, *Quantum theory of the electron liquid* (Cambridge University Press, Cambridge, 2005).
  - [26] G. E. Volovik, *Soviet Journal of Experimental and Theoretical Physics Letters* **55**, 368 (1992).

- [27] G. E. Volovik, *Soviet Physics - JETP (English Translation)*, **67**, 1804 (1988).
- [28] J. Goryo and K. Ishikawa, *Physics Letters A* **246**, 549 (1998).
- [29] M. Stone and R. Roy, *Phys. Rev. B* **69**, 184511 (2004).
- [30] H. S. Bennett and E. A. Stern, *Physical Review* **137**, A448 (1965).
- [31] I. Souza and D. Vanderbilt, *Physical Review B* **77**, 054438 (2008).
- [32] D. J. Thouless, M. Kohmoto, M. P. Nightingale, and M. den Nijs, *Phys. Rev. Lett.* **49**, 405 (1982).
- [33] E. Taylor and C. Kallin, *Phys. Rev. Lett.* **108**, 157001 (2012).
- [34] W. Huang, E. Taylor, and C. Kallin, *Phys. Rev. B* **90**, 224519 (2014).
- [35] W. Huang, S. Lederer, E. Taylor, and C. Kallin, *Phys. Rev. B* **91**, 094507 (2015).
- [36] J. J. Kinnunen, Z. Wu, and G. M. Bruun, *Phys. Rev. Lett.* **121**, 253402 (2018).
- [37] N. Luick, L. Sobirey, M. Bohlen, V. P. Singh, L. Mathey, T. Lompe, and H. Moritz, “An ideal josephson junction in an ultracold two-dimensional fermi gas,” (2019), arXiv:1908.09776 [cond-mat.quant-gas].
- [38] L. Sobirey, N. Luick, M. Bohlen, H. Biss, H. Moritz, and T. Lompe, “Observation of superfluidity in a strongly correlated two-dimensional fermi gas,” (2020), arXiv:2005.07607 [cond-mat.quant-gas].
- [39] M. G. Ries, A. N. Wenz, G. Zürn, L. Bayha, I. Boettcher, D. Kedar, P. A. Murthy, M. Neidig, T. Lompe, and S. Jochim, *Phys. Rev. Lett.* **114**, 230401 (2015).
- [40] P. Pieri, L. Pisani, and G. C. Strinati, *Phys. Rev. B* **72**, 012506 (2005).
- [41] G. Mahan, *Many-Particle Physics* (Kluwer Academic/Plenum Publishers, 2000).

## Appendix A: Calculation of the superfluid transition temperature

Here, we outline the calculation of the superfluid transition temperature for the 2D  $^{173}\text{Yb}$  gas immersed in a 3D  $^7\text{Li}$  BEC. First, we solve the following frequency-

dependent gap equation at a finite temperature  $T$  [36]

$$\Delta(\mathbf{p}, i\omega_n) = -T \sum_m \int \frac{d\mathbf{q}}{(2\pi)^2} V_{\text{ind}}(\mathbf{p} - \mathbf{q}, i\omega_n - i\omega_m) \times \frac{\Delta(\mathbf{q}, i\omega_m)}{\omega_m^2 + \mathcal{E}^2(\mathbf{q}, i\omega_m)}, \quad (\text{A1})$$

where  $\mathcal{E}(\mathbf{q}, i\omega_m) = \sqrt{\xi_{\mathbf{q}}^2 + |\Delta(\mathbf{q}, i\omega_m)|^2}$ . Here the frequency-dependent induced interaction  $V_{\text{ind}}(\mathbf{q}, i\omega_\nu)$  is given by

$$V_{\text{ind}}(\mathbf{q}, i\omega_\nu) = -n_B m_B g^2 \left[ \left( \frac{1}{\kappa_+} + \frac{1}{\kappa_-} \right) + \frac{1}{\sqrt{1 - (\omega_\nu/g_B n_B)^2}} \left( \frac{1}{\kappa_+} - \frac{1}{\kappa_-} \right) \right], \quad (\text{A2})$$

where  $\kappa_\pm = \sqrt{2m_B g_B n_B \left[ 1 \pm \sqrt{1 - (\omega_\nu/g_B n_B)^2} \right] + \mathbf{q}^2}$ .

Along with a number equation, this constitutes the Eliashberg equations of the superfluid [41].

Since the Fermi system is 2D, the superfluid transition is driven by vortex-antivortex proliferation and the critical temperature  $T_{\text{BKT}}$  is determined by the Kosterlitz-Thouless condition [7]

$$T_{\text{BKT}} = \frac{\pi}{8m_F^2} \rho_s (\{\Delta(i\omega_n)\}, T_{\text{BKT}}). \quad (\text{A3})$$

Here,  $\rho_s$  is the superfluid mass density and is a function of the gap parameters and the temperature. Neglecting the renormalisation of the interaction between vortex pairs,  $\rho_s$  can be estimated as

$$\rho_s = \rho_0 + \frac{T}{2} \sum_n \int \frac{d\mathbf{p}}{(2\pi)^2} p^2 \frac{\mathcal{E}^2(\mathbf{p}, i\omega_n) - \omega_n^2}{[\omega_n^2 + \mathcal{E}^2(\mathbf{p}, i\omega_n)]^2}, \quad (\text{A4})$$

where  $\rho_0 = m_F n_F$ . Solving Eq. (A3) self-consistently using Eqs. (A4) and the frequency-dependent gap parameters obtained from Eq. (A1), we obtain the superfluid transition temperatures shown in the main text.